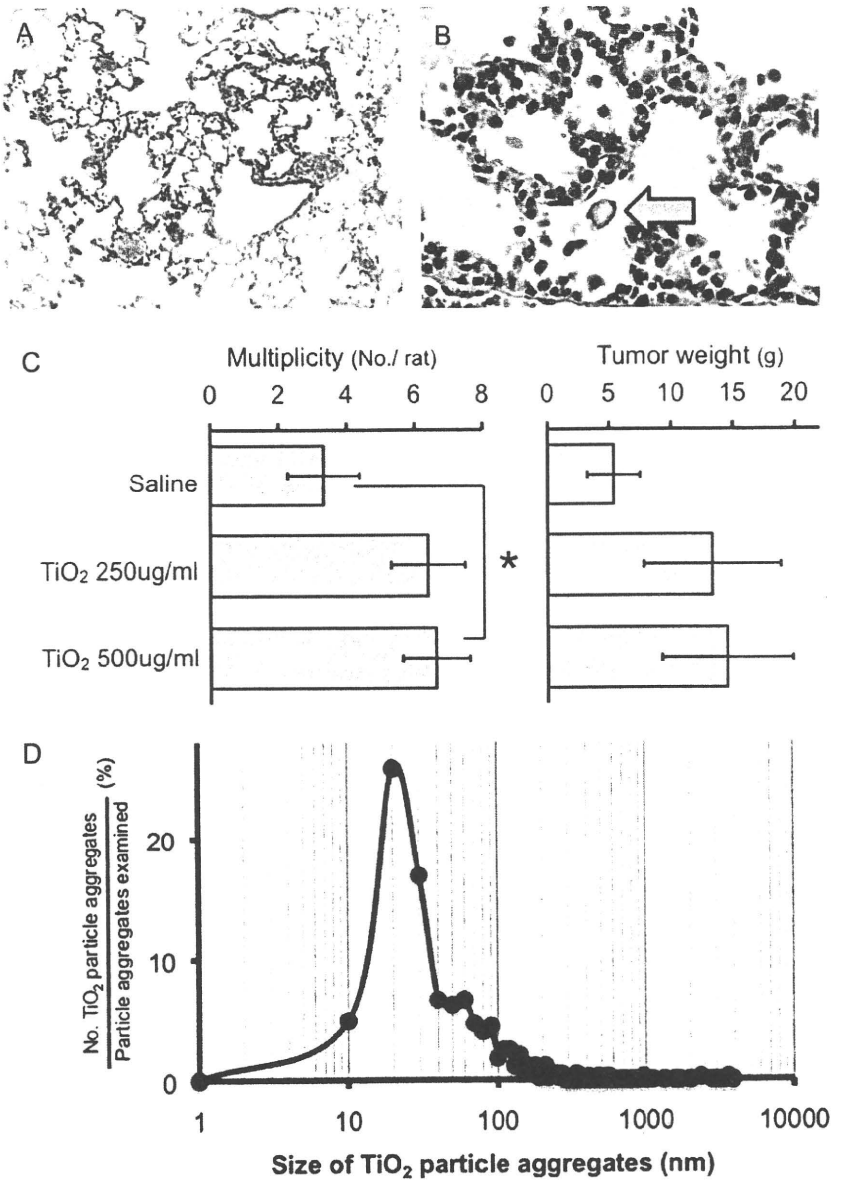


**Fig. 1.** Promoting effects of $TiO_2$ particles in DHPN-induced lung and mammary carcinogenesis (**A**) Alveolar hyperplasias observed in the lung of an H*ras*128 rat receiving DHPN and 500 μg/ml $TiO_2$ particles. (**B**) Alveolar macrophages with $TiO_2$ particles were also observed in hyperplasia lesions. (**C**) IPS of $TiO_2$ particles significantly increased the multiplicity of adenocarcinomas in the mammary gland and tended to increase the size of mammary tumors. (**D**) The size distribution of $TiO_2$ particle aggregates; among 452 particle aggregates examined, 362 (80.1%) were nanosize, i.e. <100 nm in diameter.

(data not shown). The macrophages were treated with $TiO_2$ particles suspended in saline (Figure 4A). $TiO_2$ induced secretion of MIP1α into the culture media (Figure 4B), and the culture medium collected from macrophages treated with $TiO_2$ particles promoted proliferation of A549 cells, whereas culture media collected from unexposed macrophages did not (Figure 4C). MIP1α neutralizing antibodies attenuated the promotion of A549 proliferation in a dose-dependent manner (Figure 4C). MIP1α-induced cell proliferation was also significantly suppressed by the ERK inhibitor PD98059 (Figure 4D). In addition, MIP1α increased ERK phosphorylation and PD98059 diminished ERK phosphorylation (Figure 4E).

We also examined the effect of MIP1α, GRO and IL-6, $H_2O_2$ and $TiO_2$ on the proliferation of A549 cells. MIP1α increased cell proliferation in a dose-dependent fashion, but GRO and IL-6 did not (supplementary Figure 3A–C is available at *Carcinogenesis* Online). $H_2O_2$ significantly suppressed cell proliferation, and antioxidant treatment diminished this suppression. Antioxidant treatment did not affect MIP1α-induced cell proliferation (supplementary Figure 3D is available at *Carcinogenesis* Online). These results suggest that ROS have no effect on tumor cell growth in this experiment.

In addition, $TiO_2$ did not directly increase proliferation of A549 cell (supplementary Figure 3E is available at *Carcinogenesis* Online).

*Mechanism analysis of the promotion of mammary carcinogenesis*

MIP1α was markedly elevated in the serum of the H*ras*128 rats treated with $TiO_2$ particles (Figure 5A). Serum levels of IL-6 were not changed by $TiO_2$ treatment and GRO was not detected in the serum

**Table I.** Effect of TiO2 on incidence and multiplicity of DHPN-induced alveolar hyperplasia and adenoma of the lung

| Treatment | No. of rats | Alveolar hyperplasia | | Lung adenoma | |
|---|---|---|---|---|---|
| | | Incidence (%) | Multiplicity ## (no./cm$^2$) | Incidence (%) | Multiplicity # (no./cm$^2$) |
| Saline | 9 | 9 (100) | 5.91 ± 1.19 | 0 | 0 |
| n$TiO_2$ 250 mg/ml | 10 | 10 (100) | 7.36 ± 0.97* | 1 (10) | 0.10 ± 0.10 |
| n$TiO_2$ 500 mg/ml | 11 | 11 (100) | 11.05 ± 0.87** | 4 (36) | 0.46 ± 0.21* |

*$P < 0.05$, **$P < 0.001$ versus saline control.
#$P < 0.05$, ##$P < 0.001$ in trend test (Spearman's rank correlation test).

(Figure 5A). MIP1α was slightly elevated in the mammary glands of these animals (Figure 5B); possibly, the elevated MIP1α detected in the mammary tissue was due to contamination by MIP1α in the serum. Recombinant MIP1α promoted the proliferation of C3 cells in a dose-dependent manner; a slight induction could be seen at a dose of 400 pg/ml and became statistically significant at the dose of 50 ng/ml (Figure 5C). Expression of CCR1, the major receptor of MIP1α, was observed in mammary tissue, and as in the lung, IPS of $TiO_2$ particles had little or no effect on CCR1 expression (data not shown). $TiO_2$ did not directly increase proliferation of C3 cells (supplementary Figure 3F is available at *Carcinogenesis* Online).

## Discussion

To elucidate the mechanism underlying rat lung carcinogenesis by $TiO_2$ inhalation, we chose IPS. Although this method may be less physiological than the aerosol inhalation system, we observed that agglomerates and aggregates of $TiO_2$ particles from nano to micro size (mean diameter 107.4 nm) were diffusely distributed throughout the lung including peripheral alveoli, and they did not cause obstruction of the terminal bronchioles. Accordingly, IPS of $TiO_2$ particles can be expected to act similarly to aerosol inhalation of $TiO_2$.

Occupational exposure limits for $TiO_2$ in 13 countries or regions are 5–20 mg/m$^3$ (20), which results in $TiO_2$ exposure limits of 0.27–1.07 mg/kg body wt/day; calculations based on the human respiratory volume. In the present study, a total of 1.75 mg was administered per rat for 12 weeks in the high-dose group, resulting in a dose of 0.104 mg/kg body wt/day. Therefore, the dose we used in the present study was lower than the occupational exposure limit.

$TiO_2$, nanoscale and larger sized is evaluated as a Group 2B carcinogen by World Health Organization/International Agency for Research on Cancer (4) based on 2 year animal aerosol inhalation studies (3). We conducted the present carcinogenesis study using a two-step initiation–promotion protocol as a surrogate for a 2 year long-term protocol. Our study demonstrated that $TiO_2$ particles increased the multiplicity of alveolar cell hyperplasia and adenoma in the two-step IPS-initiation–promotion protocol. We used these lesions as endpoints in carcinogenicity testing because chemically induced tumors appear to be derived from hyperplasic lesions that progress to adenoma and carcinoma (21).

Several bioassay protocols based on the two-step carcinogenesis theory have been developed as practical and sensitive assays, and the compounds that exhibit promotion activity are considered to be carcinogens (22–29). Thus, our experimental design may be a practical surrogate for the long-term lung carcinogenesis protocol.

It should be noted that proliferative lesions including alveolar cell hyperplasia and adenomas were not found in the groups subjected to $TiO_2$ particle administration without prior treatment of DHPN. This is due to the weak carcinogenic potential and short duration of exposure to $TiO_2$ particles. Using the two-step IPS-initiation–promotion protocol, however, we did observe carcinogenic activity by this weak carcinogen. Thus, the two-step IPS-initiation–promotion protocol is an appropriate system to study carcinogenesis of $TiO_2$ particles and approximates long-term $TiO_2$ inhalation studies (3,11).

We next conducted a mechanism analysis of $TiO_2$ particle carcinogenesis focusing on the initial events induced by exposure to $TiO_2$ particles. Treatment with $TiO_2$ resulted in a modest infiltration of inflammatory cells into the alveolar space and septal wall, but the primary effect was a marked increase in the number of macrophages in the alveoli, and many of these macrophages contained phagocytosed $TiO_2$ particles. Alveolar macrophages play an important role in deposition and clearance of mineral fibers/particles, and macrophage activity is known to be strongly associated with inflammatory reactions and carcinogenesis caused by fibers and particles in the lung, including asbestos (30–33). ROS are known to be produced by macrophages upon particle phagocytosis (34,35). Clinical and experimental studies indicate that ROS production and resultant oxidative stress play an important role in cellular and tissue damage, inflammation and fibrosis in the lung. In our study, a significant increase in the activity of SOD and 8-OHdG formation in the lung were observed, indicating increased ROS production and DNA damage. Because macrophages are unable to detoxify $TiO_2$ particles, the reaction against these particles would be continuous over an extended period of time. This condition is associated with high levels of ROS production (36) and tissue toxicity (37).

Cytokine analysis of the lung tissue indicated that among the 12 cytokines examined, expression of IL-6, GRO and MIP1α were significantly higher in the $TiO_2$-treated group than in the vehicle group (supplementary Table 1 is available at *Carcinogenesis* Online). IL-6 is a pro-inflammatory cytokine that is involved in host defense as well as cancer development (38,39). IL-6 has been shown to be increased in lung tumor tissue (40,41) and in the sera of lung cancer patients (42). GRO, a member of the CXC chemokine family, has been shown to be involved in inflammatory responses, chemoattraction (43), carcinogenesis (44,45) and tumor progression (46). Thus, IL-6 and GRO may be involved in the promotion of lung carcinogenesis by $TiO_2$ (47).

Of the three cytokines induced by exposure to $TiO_2$ particles, however, we were particularly interested in MIP1α. This cytokine was not only induced in the lung tissue of $TiO_2$-treated rats, but, unlike IL-6 and GRO, it was also found in the serum of these animals. MIP1α is a member of the CC chemokine family and is primarily associated with cell adhesion and migration (17), proliferation and survival of myeloma cells (48). It is produced by macrophages in response to a variety of mineral particle-induced inflammatory stimuli (18). Our results indicate that expression of MIP1α by alveolar macrophages enhances the proliferation of A549 cells. Expression of CCR1, the major receptor of MIP1α, was observed in the lung tissue, rendering lung cells receptive to MIP1α induction of proliferation. Lung damage and inflammation induced by $TiO_2$ particles has also been reported to be associated with increased cell proliferation of lung epithelium cells (49), which is consistent with our results.

The MEK1–ERK-signaling pathway has been shown to be involved in CCR1 signaling (48). In the present study, the MEK1-specific inhibitor PD98059 suppressed MIP1α-induced cell proliferation and ERK phosphorylation. These results suggest that MEK1 is one of the downstream signaling molecules of MIP1α and the MEK1–ERK-signaling pathway may be partially involved in MIP1α signaling.

It should be noted that, in our IPS-initiation–promotion protocol, $TiO_2$ exposure also promoted DHPN-initiated mammary carcinogenesis. Our results suggest that MIP1α secreted by alveolar macrophages and transported via the circulatory system caused

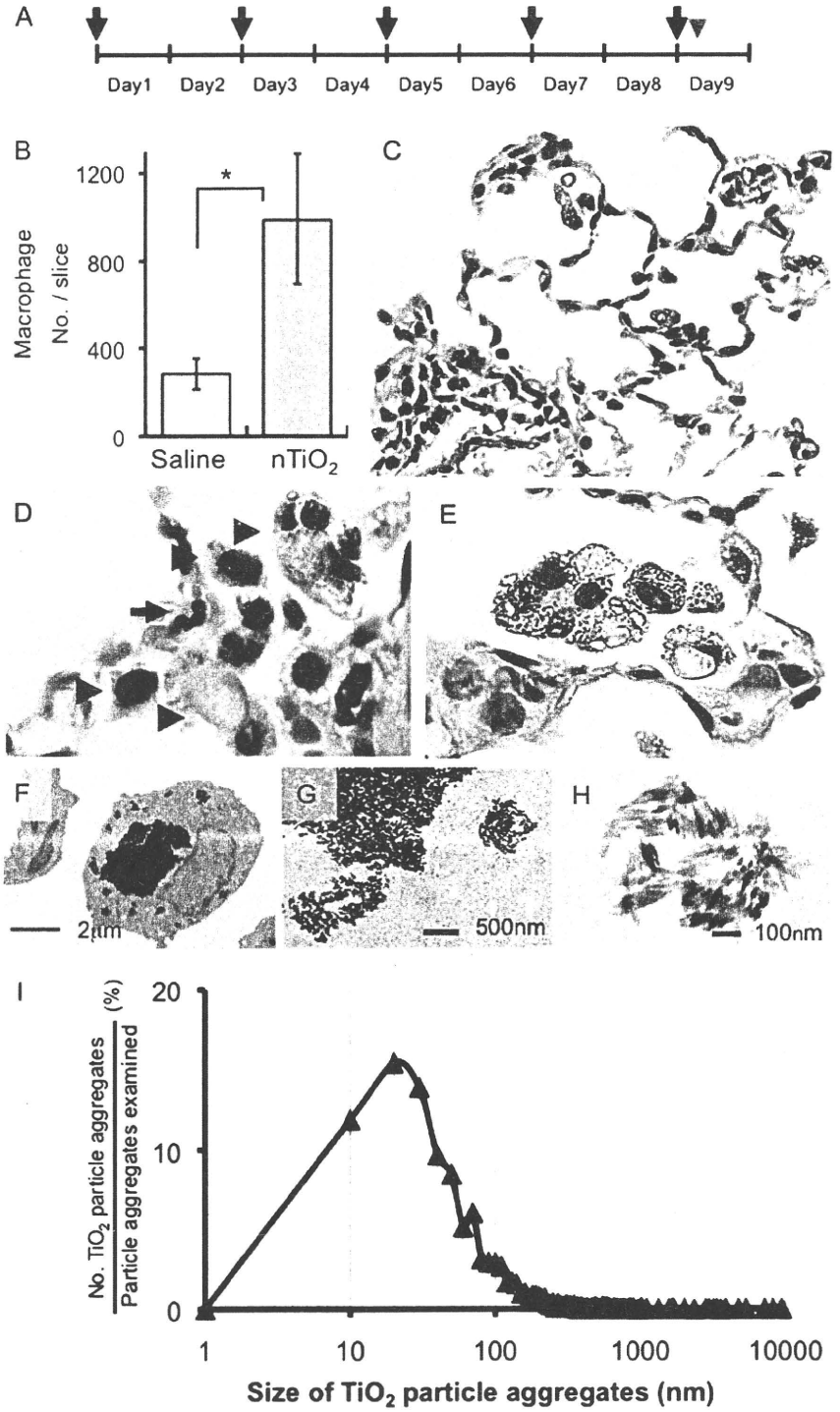


**Fig. 2.** $TiO_2$ particles in alveolar macrophages by light and electron microscopy (**A**) Twenty female SD rats (wild-type counterpart of H*ras*128) aged 10 weeks were treated by IPS with 0.5 ml suspension of 500 μg/ml $TiO_2$ particles in saline five times over a 9 day period. Arrows and arrowhead indicates IPS treatment and killing of the animals, respectively. (**B**) IPS of $TiO_2$ particles significantly increased the number of macrophages in the alveoli. (**C**) Inflammatory reactions were observed in the lung with slight infiltration of macrophages, neutrophils and lymphocytes. (**D**) $TiO_2$ particles were observed in alveolar macrophages (hematoxylin and eosin staining). Arrowheads indicate macrophages and the smaller cell indicated by the arrow is a neutrophil with its characteristic multilobular nucleus. (**E**) The multinucleated cells containing these particles were positive for the macrophage marker CD68 (Alkaline phosphatase reaction, red color). (**F**) TEM findings showed that $TiO_2$ particles of various sizes (~50 nm to 5 μm) were observed phagocytosed by alveolar macrophages. (**G**) Electron dense bodies were aggregates of $TiO_2$ particles. (**H**) TEM findings of $TiO_2$ particles in saline suspension before IPS. The shape of the $TiO_2$ particle aggregates was similar to those observed in macrophages. (**I**) The size distribution of $TiO_2$ particle aggregates: of 2571 particle aggregates examined, 1970 (77.1%) were <100 nm. The average size was 107.4 nm and the median size was 48.1 nm.

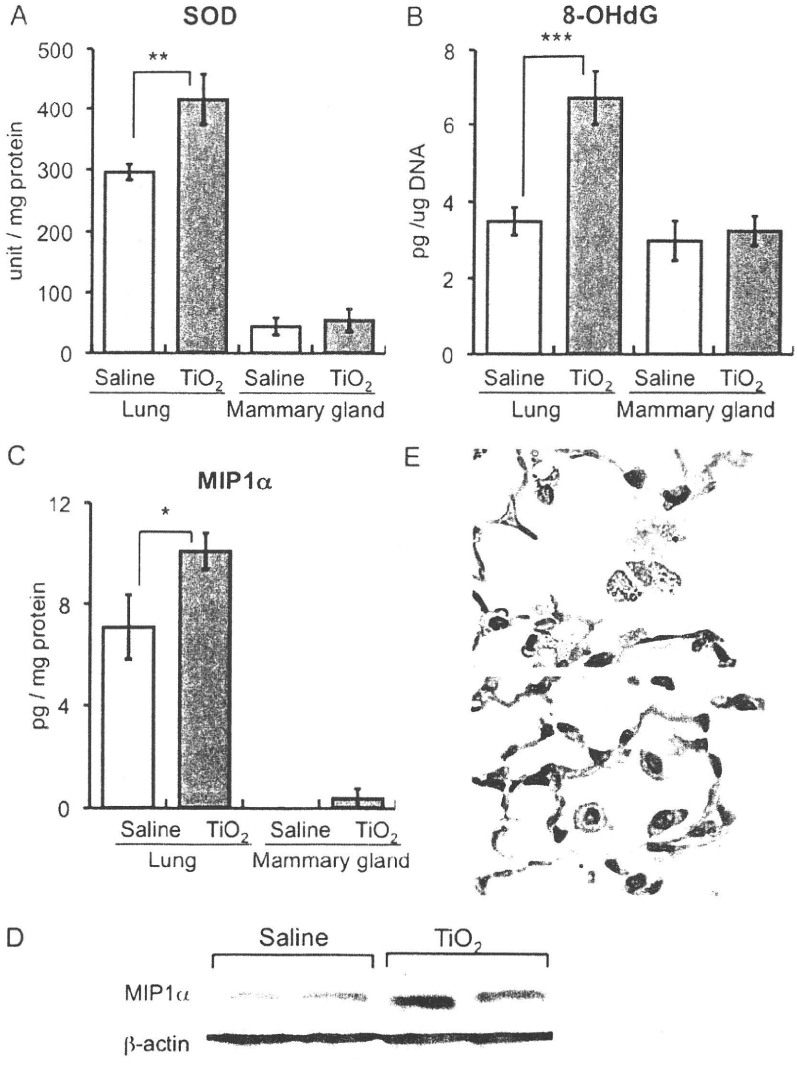


**Fig. 3.** Inflammatory factors upregulated in the lungs of wild-type rats by IT-spraying of $TiO_2$ particles in the IPS 9 day study (**A**) SOD activity and (**B**) 8-OHdG level in wild-type rats treated with $TiO_2$ particles or saline. (**C**) MIP1α protein level was significantly increased (142%) in the lung tissue of wild-type rats treated with $TiO_2$ (suspension array analysis). MIP1α was detected in the mammary gland of the $TiO_2$ group but not in the vehicle group. (**D**) In western blotting, expression of MIP1α was increased in the $TiO_2$ group compared with vehicle group. (**E**) MIP1α was immunohistochemically detected in alveolar macrophages containing $TiO_2$ particles (upper) but was not detected in macrophages of rats that were not exposed to $TiO_2$ particles (lower).

proliferation of mammary epithelial cells and thereby promoted mammary carcinogenesis. As with the lung, CCR1 was expressed by mammary cells, rendering these cells receptive to MIP1α induction of proliferation. While MIP1α secreted by alveolar macrophages would be diluted by the blood volume and while these levels may not be high enough to increase mammary cell proliferation in a short *in vitro* proliferation assay; it is possible that continuous low level stimulation over the course of 12 weeks could increase mammary cell proliferation in the environment of the mammary gland *in vivo*. Another possibility is that $TiO_2$ particles may act directly on the mammary gland after translocation to the mammary gland from the lung. However, $TiO_2$ exposure of mammary carcinoma cells did not induce proliferation *in vitro*. It must be understood that promotion of DHPN-induced mammary carcinogenesis by $TiO_2$ particles was observed in H*ras*128 female rats, and these animals are very highly susceptible to mammary carcinogenesis (50). Although, the effects we observed on promotion of mammary carcinogenesis in these animals may not be directly relevant to most humans, people at high risk for mammary carcinogenesis, such as individuals harboring BRCA mutations, may be a relevant population as regards the risk presented by nanoscale $TiO_2$.

Although our observations are based on results obtained with a mixed population of nanoscale and larger sized particle aggregates, size analysis indicated that 80.1% of them were nanoscale (<100 nm in diameter) in the 16 week IPS-initiation–promotion study and 76.6% were nanoscale in the IPS 9 day study. Thus, the results can be interpreted as being strongly associated with nanoscale particle aggregates.

In conclusion, the IPS-initiation–promotion protocol detected $TiO_2$ carcinogenic activity in the rat lung and is therefore comparable, at least for $TiO_2$ inhalation, to a long-term whole body inhalation carcinogenesis study. We also elucidated a plausible mechanism for the carcinogenic effect of $TiO_2$ particles in the rat lung. Phagocytosis of $TiO_2$ particles by alveolar macrophages resulted in ROS production and DNA damage and increased expression of MIP1α. MIP1α in turn was able to enhance proliferation of lung epithelium cells. Thus, lung

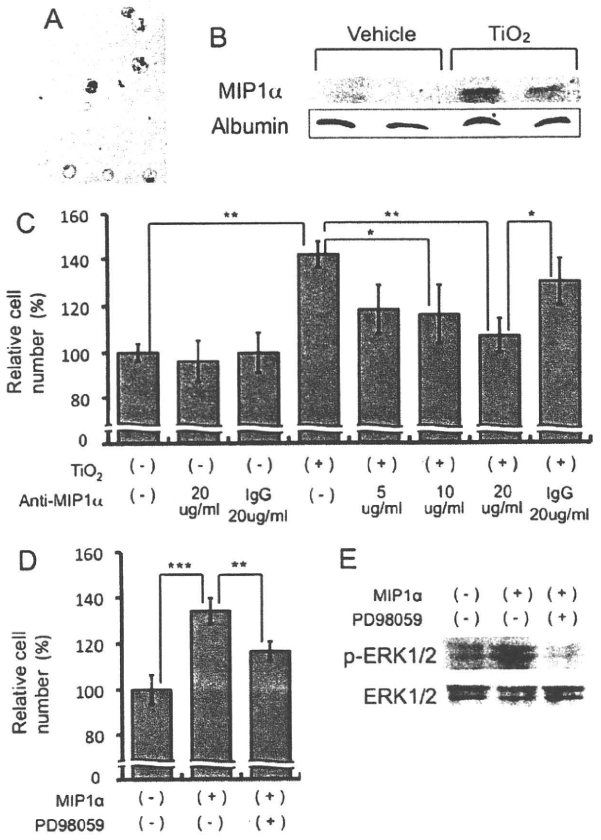


**Fig. 4.** Growth stimulation effects of conditioned medium from alveolar macrophages on human lung cancer cell lines. (**A**) Primary cultured alveolar macrophages of rats were treated with $TiO_2$ particles. (**B**) MIP1α was detected in the culture medium. (**C**) The number of A549 cells was significantly increased by addition of conditioned medium from alveolar macrophages treated with $TiO_2$ particles. MIP1α neutralizing antibody attenuated this effect in a dose-dependent manner. Irrelevant IgG was used as control antibody. (**D**) MIP1α-induced cell proliferation was significantly suppressed by the ERK inhibitor PD98059. (**E**) MIP1α increased ERK phosphorylation and PD98059 diminished this phosphorylation.

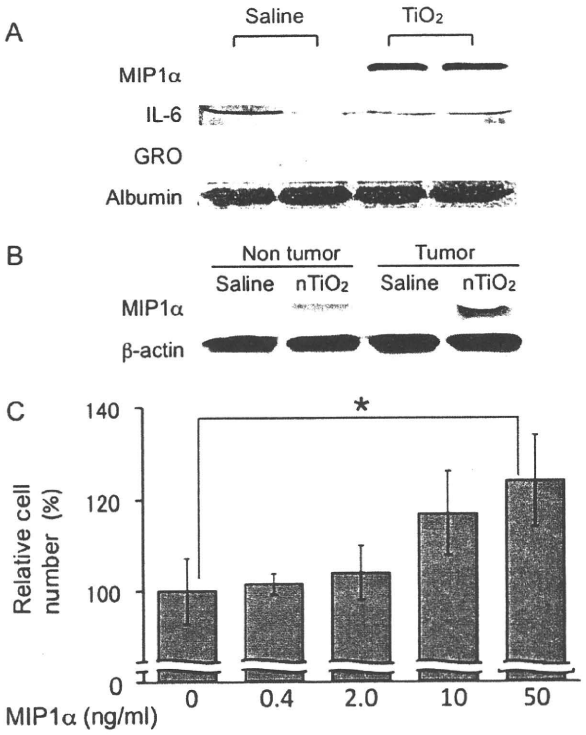


**Fig. 5.** Promotion effects of MIP1α on proliferation of a rat mammary cancer cell line, C3 (**A**) MIP1α was detected in the serum of the H*ras*128 rats treated with $TiO_2$ but not in vehicle control rats in the 16 week study. No difference in IL-6 in the serum was observed and GRO was not detected in the serum. (**B**) MIP1α levels are slightly elevated in non-tumor and tumor tissue of the mammary gland of animals treated by IPS with $TiO_2$ particles in the 16 week study. (**C**) Recombinant MIP1α increased the number of rat mammary carcinoma C3 cells in a dose-dependent manner ($P = 0.0127$).

tissue exposed to $TiO_2$ particles exhibits increase in both DNA damage and proliferation. Importantly, a similar mechanism would function in humans in the promotion of lung carcinogenesis associated with inhalation of $TiO_2$ particles and other nanoparticles with the capacity to form aggregates. In addition, $TiO_2$ administered to the lung had carcinogenic activity in the H*ras*128 transgenic rat mammary gland; this carcinogenic activity is probably mediated via serum MIP1α resulting from expression of MIP1α by alveolar macrophages. This finding may indicate that exposure of $TiO_2$ particles is a risk factor for mammary carcinogenesis in predisposed populations, such as individuals with BRCA mutations.

## Supplementary material

Supplementary Figures 1–3 and Tables 1 and 2 can be found at http://carcin.oxfordjournals.org/

## Funding

Health and Labour Sciences Research Grants, Ministry of Health, Labour and Welfare, Japan (Research on Risk of Chemical Substance 21340601, H18-kagaku-ippan-007); a grant-in-aid for the Second Term Comprehensive 10 Year Strategy for Cancer Control, Ministry of Health, Labour and Welfare, Japan; grants-aid for Cancer Research, Ministry of Education, Culture, Sports, Science and Technology.

## Acknowledgements

*Conflict of Interest Statement:* None declared.

## References

1. Oberdorster,G. (2002) Toxicokinetics and effects of fibrous and nonfibrous particles. *Inhal. Toxicol.*, **14**, 29–56.
2. Romundstad,P. *et al.* (2001) Cancer incidence among workers in the Norwegian silicon carbide industry. *Am. J. Epidemiol.*, **153**, 978–986.
3. Pott,F. *et al.* (2005) Carcinogenicity study with nineteen granular dusts in rats. *Eur. J. Oncol.*, **10**, 249–281.
4. Baan,R. *et al.* (2006) Carcinogenicity of carbon black, titanium dioxide, and talc. *Lancet Oncol.*, **7**, 295–296.
5. Schulte,P. *et al.* (2008) Occupational risk management of engineered nanoparticles. *J. Occup. Environ. Hyg.*, **5**, 239–249.
6. Maynard,A.D. *et al.* (2006) Safe handling of nanotechnology. *Nature*, **444**, 267–269.
7. Scheringer,M. (2008) Nanoecotoxicology: environmental risks of nanomaterials. *Nat. Nanotechnol.*, **3**, 322–323.
8. Borm,P. *et al.* (2006) Research strategies for safety evaluation of nanomaterials, part V: role of dissolution in biological fate and effects of nanoscale particles. *Toxicol. Sci.*, **90**, 23–32.
9. Phalen,R.F. (1976) Inhalation exposure of animals. *Environ. Health Perspect.*, **16**, 17–24.

10. Mauderly,J.L. (1997) Relevance of particle-induced rat lung tumors for assessing lung carcinogenic hazard and human lung cancer risk. *Environ. Health Perspect.*, **105** (suppl. 5), 1337–1346.
11. Roller,M. *et al.* (2006) Lung tumor risk estimates from rat studies with not specifically toxic granular dusts. *Ann. N. Y. Acad. Sci.*, **1076**, 266–280.
12. Imaida,K. *et al.* (1996) Initiation-promotion model for assessment of carcinogenicity: medium-term liver bioassay in rats for rapid detection of carcinogenic agents. *J. Toxicol. Sci.*, **21**, 483–487.
13. IARC (1999) The use of short-and medium-term tests for carcinogens and data on genetic effects in carcinogenic hazard evaluation. Consensus report. *IARC Sci. Publ.*, **146**, 1–18.
14. Asamoto,M. *et al.* (2000) Transgenic rats carrying human c-Ha-ras proto-oncogenes are highly susceptible to N-methyl-N-nitrosourea mammary carcinogenesis. *Carcinogenesis*, **21**, 243–249.
15. Han,B.S. *et al.* (2002) Inhibitory effects of 17beta-estradiol and 4-n-octylphenol on 7,12-dimethylbenz[a]anthracene-induced mammary tumor development in human c-Ha-ras proto-oncogene transgenic rats. *Carcinogenesis*, **23**, 1209–1215.
16. Ohnishi,T. *et al.* (2007) Possible application of human c-Ha-ras proto-oncogene transgenic rats in a medium-term bioassay model for carcinogens. *Toxicol. Pathol.*, **35**, 436–443.
17. Terpos,E. *et al.* (2005) Significance of macrophage inflammatory protein-1 alpha (MIP-1alpha) in multiple myeloma. *Leuk. Lymphoma*, **46**, 1699–1707.
18. Driscoll,K.E. *et al.* (1993) Macrophage inflammatory proteins 1 and 2: expression by rat alveolar macrophages, fibroblasts, and epithelial cells and in rat lung after mineral dust exposure. *Am. J. Respir. Cell Mol. Biol.*, **8**, 311–318.
19. Hamaguchi,T. *et al.* (2006) Establishment of an apoptosis-sensitive rat mammary carcinoma cell line with a mutation in the DNA-binding region of p53. *Cancer Lett.*, **232**, 279–288.
20. IARC (1989) Titanium dioxide. *IARC monograph Evaluation of carcinogenic risks to humans*. IARC Scientific Publications, Lyon. vol. 47, pp. 307–326.
21. Stoner,G.D. *et al.* (1993) Lung tumors in strain A mice: application for studies in cancer chemoprevention. *J. Cell. Biochem. Suppl.*, **17F**, 95–103.
22. Pitot,H.C. *et al.* (1978) Biochemical characterisation of stages of hepatocarcinogenesis after a single dose of diethylnitrosamine. *Nature*, **271**, 456–458.
23. Peraino,C. *et al.* (1971) Reduction and enhancement by phenobarbital of hepatocarcinogenesis induced in the rat by 2-acetylaminofluorene. *Cancer Res.*, **31**, 1506–1512.
24. Ito,N. *et al.* (2003) A medium-term rat liver bioassay for rapid *in vivo* detection of carcinogenic potential of chemicals. *Cancer Sci.*, **94**, 3–8.
25. Ito,N. *et al.* (1988) Wide-spectrum initiation models: possible applications to medium-term multiple organ bioassays for carcinogenesis modifiers. *Jpn. J. Cancer Res.*, **79**, 413–417.
26. IARC (1980) Long-term and short-term screening assays for carcinogens: a critical appraisal. *IARC Scientific Publications, Lyon, vol.* 83 (suppl. 2), pp. 1–146.
27. Konishi,Y. *et al.* (1987) Lung carcinogenesis by N-nitrosobis(2-hydroxypropyl)amine-related compounds and their formation in rats. *IARC Sci. Publ.*, **82**, 250–252.
28. Nishikawa,A. *et al.* (1994) Effects of cigarette smoke on N-nitrosobis(2-oxopropyl)amine-induced pancreatic and respiratory tumorigenesis in hamsters. *Jpn. J. Cancer Res.*, **85**, 1000–1004.
29. Yamanaka,K. *et al.* (1996) Exposure to dimethylarsinic acid, a main metabolite of inorganic arsenics, strongly promotes tumorigenesis initiated by 4-nitroquinoline 1-oxide in the lungs of mice. *Carcinogenesis*, **17**, 767–770.
30. Rom,W.N. *et al.* (1991) Cellular and molecular basis of the asbestos-related diseases. *Am. Rev. Respir. Dis.*, **143**, 408–422.
31. Heppleston,A.G. (1984) Pulmonary toxicology of silica, coal and asbestos. *Environ. Health Perspect.*, **55**, 111–127.
32. Renwick,L.C. *et al.* (2001) Impairment of alveolar macrophage phagocytosis by ultrafine particles. *Toxicol. Appl. Pharmacol.*, **172**, 119–127.
33. Rimal,B. *et al.* (2005) Basic pathogenetic mechanisms in silicosis: current understanding. *Curr. Opin. Pulm. Med.*, **11**, 169–173.
34. Wang,Y. *et al.* (2007) The role of the NADPH oxidase complex, p38 MAPK, and Akt in regulating human monocyte/macrophage survival. *Am. J. Respir. Cell Mol. Biol.*, **36**, 68–77.
35. Bhatt,N.Y. *et al.* (2002) Macrophage-colony-stimulating factor-induced activation of extracellular-regulated kinase involves phosphatidylinositol 3-kinase and reactive oxygen species in human monocytes. *J. Immunol.*, **169**, 6427–6434.
36. Dorger,M. *et al.* (2000) Comparison of the phagocytic response of rat and hamster alveolar macrophages to man-made vitreous fibers *in vitro*. *Hum. Exp. Toxicol.*, **19**, 635–640.
37. Blake,T. *et al.* (1998) Effect of fiber length on glass microfiber cytotoxicity. *J. Toxicol. Environ. Health A*, **54**, 243–259.
38. Kabir,S. *et al.* (1995) Serum levels of interleukin-1, interleukin-6 and tumour necrosis factor-alpha in patients with gastric carcinoma. *Cancer Lett.*, **95**, 207–212.
39. Schneider,M.R. *et al.* (2000) Interleukin-6 stimulates clonogenic growth of primary and metastatic human colon carcinoma cells. *Cancer Lett.*, **151**, 31–38.
40. Asselin-Paturel,C. *et al.* (1998) Quantitative analysis of Th1, Th2 and TGF-beta1 cytokine expression in tumor, TIL and PBL of non-small cell lung cancer patients. *Int. J. Cancer*, **77**, 7–12.
41. Matanic,D. *et al.* (2003) Cytokines in patients with lung cancer. *Scand. J. Immunol.*, **57**, 173–178.
42. Brichory,F.M. *et al.* (2001) An immune response manifested by the common occurrence of annexins I and II autoantibodies and high circulating levels of IL-6 in lung cancer. *Proc. Natl Acad. Sci. USA*, **98**, 9824–9829.
43. Rollins,B.J. (1997) Chemokines. *Blood*, **90**, 909–928.
44. Zhou,Y. *et al.* (2005) The chemokine GRO-alpha (CXCL1) confers increased tumorigenicity to glioma cells. *Carcinogenesis*, **26**, 2058–2068.
45. Yang,G. *et al.* (2006) The chemokine growth-regulated oncogene 1 (Gro-1) links RAS signaling to the senescence of stromal fibroblasts and ovarian tumorigenesis. *Proc. Natl Acad. Sci. USA*, **103**, 16472–16477.
46. Li,A. *et al.* (2004) Constitutive expression of growth regulated oncogene (gro) in human colon carcinoma cells with different metastatic potential and its role in regulating their metastatic phenotype. *Clin. Exp. Metastasis*, **21**, 571–579.
47. Rollins,B.J. (2006) Inflammatory chemokines in cancer growth and progression. *Eur. J. Cancer*, **42**, 760–767.
48. Lentzsch,S. *et al.* (2003) Macrophage inflammatory protein 1-alpha (MIP-1 alpha) triggers migration and signaling cascades mediating survival and proliferation in multiple myeloma (MM) cells. *Blood*, **101**, 3568–3573.
49. Baggs,R.B. *et al.* (1997) Regression of pulmonary lesions produced by inhaled titanium dioxide in rats. *Vet. Pathol.*, **34**, 592–597.
50. Tsuda,H. *et al.* (2001) High susceptibility of transgenic rats carrying the human c-Ha-ras proto-oncogene to chemically-induced mammary carcinogenesis. *Mutat. Res.*, **477**, 173–182.

*Received September 27, 2009; revised January 14, 2010; accepted January 24, 2010*

# Biodegradation of $C_{60}$ Fullerene Nanowhiskers by Macrophage-like Cells

SHIN-ICHI NUDEJIMA, KUN'ICHI MIYAZAWA
Fullerene Engineering Group, Exploratory Nanotechnology Research Laboratory
National Institute for Materials Science (NIMS)
1-1 Namiki, Tsukuba, Ibaraki, 305-0044
JAPAN
JUNKO OKUDA-SHIMAZAKI, AKIYOSHI TANIGUCHI
Advanced Medical Material Group, Biomaterials Center
National Institute for Materials Science (NIMS)
1-1 Namiki, Tsukuba, Ibaraki, 305-0044
JAPAN
NUDEJIMA.Shinichi@nims.go.jp http://www.nims.go.jp/fullerene/index/index.html

*Abstract:* To evaluate the biological impact of $C_{60}$ fullerene nanowhiskers ($C_{60}$NWs), an interaction between phorbol 12-myristate 13-acetate (PMA)-treated THP-1 cells (macrophage-like cells) and the $C_{60}$NWs was investigated in this study. The macrophage-like cells were exposed to 10 μg/mL of $C_{60}$NWs with an average length of about 6.0 μm and an average diameter of 660 nm. After 1, 3, 6, 12, 24 and 48 h of the exposure, the cells were fixed, stained with Hoechst 33342 and rhodamine-phalloidin and were observed by a differential interference contrast and confocal laser scanning microscope to estimate an uptake rate of $C_{60}$NWs into cells. To assess the biodegradability of $C_{60}$NWs by the macrophage-like cells, the cells and the exposed $C_{60}$NWs were observed by an inverted optical phase-contrast microscope for 28 days after the exposure. After the long-term co-culture of cells and $C_{60}$NWs, the cells were decomposed by proteinase K and the exposed $C_{60}$NWs were observed with an optical microscope and a scanning electron microscope to examine the change of $C_{60}$NWs by the cells. The macrophage-like cells internalized the $C_{60}$NWs with time and more than 70% of the cells internalized the $C_{60}$NWs after 48-h exposure. After the long-term co-culture, decomposed $C_{60}$NWs were observed in the cells and the number of short (less than 3.0 μm in length) $C_{60}$NWs increased after the exposure. These results suggest that macrophages may be able to decompose $C_{60}$NWs into $C_{60}$ molecules as the primary immune response.

*Key-Words:Fullerene nanowhisker, Needle-like crystal, Biodegradation, Macrophage, Biological assessment, In vitro*

## 1 Introduction

Nanomaterials possess enormous potential for wide application in various fields owing to their unique properties and some of them have already been used in daily life. Fullerene nanowhiskers (FNWs), one of the most promising nanomaterials, have needle-like structures, and are composed of the fullerene molecules that are usually bonded via van der Waals forces and are synthesized by the liquid-liquid interfacial precipitation method [1]. The FNWs are expected for various applications such as low-dimensional semiconductors, field emission tips, nanoprobes for microdevices, fiber-reinforced nanocomposites, composite elements for lubrication, and so on. But the biological impact of FNWs is not clear and should be studied before their practical use.

Carbon nanotubes (CNTs), one of the most promising nanomaterials, have also the needle-like structure like FNWs. Long CNTs may be hazardous to health and environment owing to their needle-like morphology and biopersistence like asbestos [2, 3]. The nanosized needle-like structure resembling asbestos has been suspected to induce the asbestosis via inhalation. Recent studies demonstrated that multiwalled carbon nanotubes (MWCNTs) reached the subpleura in mice after the inhalation administration of MWCNTs [4]. By the exposure of mesothelioma lining of the body cavity of mice to MWCNTs, an asbestos-like pathogenic behavior associated with CNTs was observed, indicating a structure-activity relationship based on the length, to which asbestos and other pathogenic fibers show [2].

It is important to know whether the needle-like nanomaterials are decomposed in organisms or not,

ISSN: 1790-5125

ISBN: 978-960-474-164-9

because the biodegradable needle-like nanomaterials are considered not to harm the organisms [3, 5]. Hence, the biodegradation properties of $C_{60}$NWs are required for the biological assessment.

Macrophages are one of the immune system cells and defend the host against the foreign substances in a nonspecific manner during the early phase of infection. THP-1 is a human acute monocytic leukemia cell line and it is well known that the THP-1 cells are induced to differentiate into macrophage-like cells by treatment with PMA [6]. In our previous pilot study, we observed the macrophage-like cells exposed to 0.1, 1 and 10 μg/mL of the $C_{60}$NWs with the average length of 6.0 μm and the average diameter of 660 nm by an inverted optical phase-contrast microscope for 48 h [7]. The macrophage-like cells were observed to internalize the $C_{60}$NWs gradually, but the exposed $C_{60}$NWs didn't affect the cellular morphology. The $C_{60}$NWs may not exert the affect which is similar to the needle-like structure if macrophages decompose them.

In this study, we estimated the uptake rate of $C_{60}$NWs by macrophage-like cells in detail and assessed the biodegradability of $C_{60}$NWs by the cells as one of the biodegradation assessments of the $C_{60}$NWs in organisms.

## 2 Materials and Methods

### 2.1 Materials

#### 2.1.1 $C_{60}$NWs

$C_{60}$NWs were synthesized by the liquid-liquid interfacial precipitation method using a $C_{60}$-saturated toluene solution and isopropyl alcohol [1, 7]. The length of $C_{60}$NWs ranged from 1 to 17 μm with an average of 6.0 μm and their diameter ranged from 300 to 1340 nm with an average of 660 nm.

#### 2.1.2 Macrophage-like cells

THP-1 cells were purchased from American Type Culture Collection (ATCC, VA, USA). The THP-1 cells were cultured in a RPMI1640 medium (Invitrogen, CA, USA) supplemented with 10% heat inactivated fetal bovine serum (FBS, JRH Biosciences, KS, USA), 100 units/mL penicillin and 100 μg/mL streptomycin (Nacalai Tesque, Japan) (culture solution) at 37°C in an atmosphere of 5% $CO_2$ and saturated humidity. The THP-1 cells were subcultured every three or four days, where the number of cells in culture was maintained by centrifugation (at 1000 rpm for 3 min) and subsequent resuspension at 2 x $10^5$ viable cells/mL. The THP-1 cells were induced to differentiate into macrophage-like cells by treatment with 10 nM of PMA (Wako Pure Chemicals, Japan) for 24 h at 37°C in an atmosphere of 5% $CO_2$ and saturated humidity [7].

### 2.2 Methods

#### 2.2.1 Exposure to $C_{60}$NWs

$C_{60}$NWs were dispersed in the culture solution with a concentration of 1 mg/mL [7]. The macrophage-like cells were exposed to the $C_{60}$NWs' suspension with the final concentration of 10 μg/mL $C_{60}$NWs that was adjusted by ultrasonic agitation.

#### 2.2.2 Phagocytosis assay of $C_{60}$NWs

2 x $10^5$ THP-1 cells were induced to differentiate into macrophage-like cells by PMA on a cover glass (12-545-85, Thermo Fisher Scientific, MA, USA) in 2 mL of culture solution inside a 35 mm polystyrene culture dish (Greiner Bio-One, Germany). The macrophage-like cells were exposed to 20 μL of the $C_{60}$NWs' suspension. After 1, 3, 6, 12, 24 and 48 h of the exposure, the macrophage-like cells were fixed by 4% paraformaldehyde (Muto Pure Chemicals, Japan) and stained with rhodamine-phalloidin (Sigma-Aldrich, MO, USA) and Hoechst 33342 (Wako Pure Chemicals, Japan). The macrophage-like cells were observed with a differential interference contrast and confocal laser scanning microscope (TCS SP5, Leica Microsystems, Germany) to locate three-dimentionally the position of $C_{60}$NWs.

#### 2.2.3 Observation of $C_{60}$NWs in Macrophage-like cells

2 x $10^5$ THP-1 cells were induced to differentiate into macrophage-like cells by PMA in 2 mL of culture solution in the 35 mm polystyrene culture dish. The macrophage-like cells were exposed to 20 μL of the $C_{60}$NWs suspension. Half of the medium was replaced by a new medium (10 nM PMA, 100 μg/mL penicillin, 100 units/mL streptomycin and 10% heat inactivated FBS in RPMI1640) every day for 28 days after the exposure for one day. The macrophage-like cells and $C_{60}$NWs were observed by an inverted optical phase-contrast microscope (DMIL-HC, Leica Microsystems, Germany) every day before the medium replacement. As a control experiment, the macrophage-like cells that were not exposed to $C_{60}$NWs and the $C_{60}$NWs in the PMA-containing medium were observed by the inverted optical phase-contrast microscope every day before the medium replacement.

#### 2.2.4 Observation of the $C_{60}$NWs after exposure

1 x $10^5$ THP-1 cells were induced to differentiate into macrophage-like cells in 1 mL of culture solution

using a cell culture insert (0.4 μm of pore size, Millipore, MA, USA) hanged from the top edge of a 6-well plate (Greiner bio-one, Germany) (Fig. 1). 4 mL medium was used (1 mL in the cell culture insert and the other 3 mL in the 6-well dish). The macrophage-like cells were exposed to 10 μL of the $C_{60}$NWs suspension. 0.5 mL of PMA-containing medium was poured into the cell culture insert after removing 0.5 mL of old medium from the 6-well plate every day for 28 days. Immediately and 28 days after the exposure, the macrophage-like cells were decomposed by 4 mL of proteinase K (Wako Pure Chemicals, Japan) with a concentration of 200 μg/mL at 50°C for 3 h after washing the cells twice with 4 mL of PBS buffer. The $C_{60}$NWs were washed with 4 mL of ultrapure water twice on the membrane of cell culture insert. The change of $C_{60}$NWs was observed with an optical microscope (ECLIPSE ME 600, Nikon, Japan) to measure the length. The morphological change of $C_{60}$NWs was observed with a scanning electron microscope (SEM, JSM-6700, JEOL, Japan) after coating the membrane of cell culture insert with Pt for 1 min by a deposition apparatus (ESC-101, ELIONIX, Japan). $C_{60}$NWs were dispersed in a PMA-containing medium as a control experiment. The change of $C_{60}$NWs was similarly observed as above.

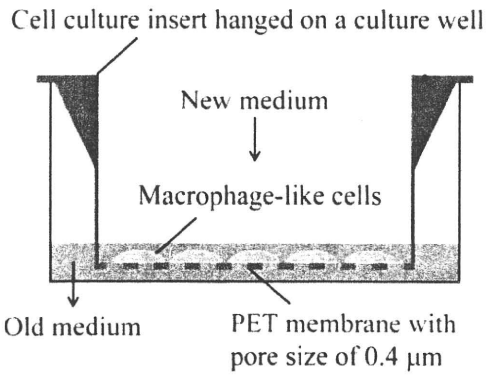


**Fig.1.** Macrophage-like cells were cultivated on a PET membrane with $C_{60}$NWs.

## 3 Results

### 3.1 Phagocytosis assay of $C_{60}$NWs

As shown in Fig. 2, the $C_{60}$NWs were phagocytized by the macrophage-like cells. The macrophage-like cells internalized the $C_{60}$NWs with time and more than 70% of the cells internalized them after 48 h exposure to 10 μg/mL of $C_{60}$NWs (Fig. 3).

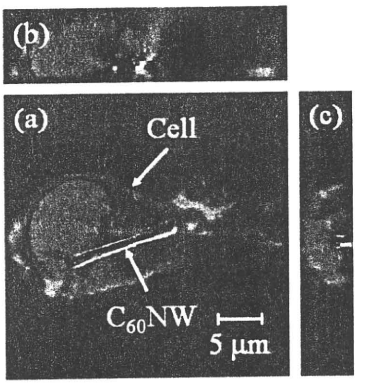


**Fig.2.** Confocal laser microscopy images with differential interference contrast of the macrophage-like cells exposed to the $C_{60}$NWs for 24 h. (a) Horizontal cross section, (b) and (c) vertical cross sections. The nucleus and F-actin are shown in blue (Hoechst 33342) and in red (rhodamine-phalloidin), respectively. The Hoechst 33342 was excited with light of 405 nm wavelength and the emission was monitored at 420-520 nm. The rhodamine-phalloidin was excited at 543 nm and the emission was monitored at 560-700 nm.

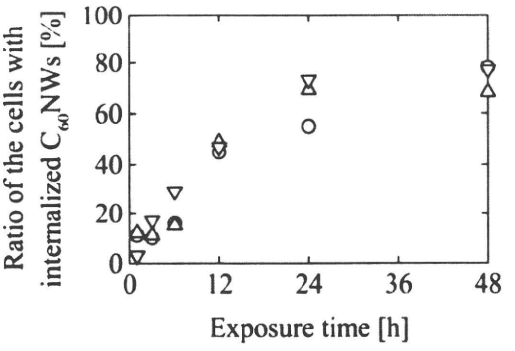


**Fig.3.** Ratio of the macrophage-like cells with internalized $C_{60}$NWs. 100 macrophage-like cells were observed for each point.

### 3.2 Biodegradation assessment of $C_{60}$NWs

After the long-term co-culture of macrophage-like cells and $C_{60}$NWs, decomposed $C_{60}$NWs were observed in the cells (Fig. 4).

A change of length distribution of $C_{60}$NWs was estimated (Fig. 5). The number of short (less than 3.0 μm in length) $C_{60}$NWs increased after the co-culture with the macrophage-like cells for 28 days (Fig. 6). In contrast, at the control experiment, an increase of the

ISSN: 1790-5125

ISBN: 978-960-474-164-9

number of short $C_{60}$NWs was not observed.

The change of $C_{60}$NWs' morphology was not observed in the medium for 28 days (Fig. 7). On the other hand, granular crystals were observed on the membrane after the co-culture of macrophage-like cells and $C_{60}$NWs for 28 days.

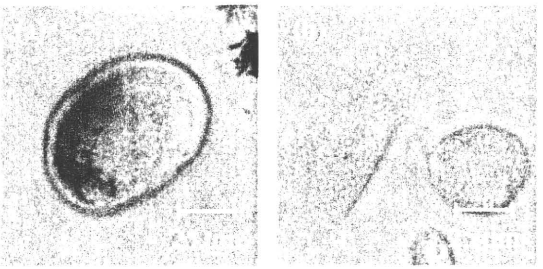

**Fig.4.** (a) Macrophage-like cells cultivated (a) with and (b) without $C_{60}$NWs for 21 days after the exposure to $C_{60}$NWs.

## 4 Discussion

### 4.1 Uptake of $C_{60}$NWs

Macrophages have a role to recognize, internalize and digest foreign materials. The uptake of foreign materials depends on their size and surface properties [8]. $C_{60}$ is phagocytized by macrophages [9] and the uptake rate of $C_{60}$ is lower than that of graphite particles [10].

The $C_{60}$NWs were also phagocytized by macrophage-like cells and the macrophage-like cells internalized the $C_{60}$NWs with time and more than 70% of the cells internalized them after 48 h of exposure to 10 μg/mL of $C_{60}$NWs. However, in our previous study, no alteration of cellular morphology was observed in the macrophage-like cells exposed to $C_{60}$NWs [7]. The macrophage-like cells were able to internalize the $C_{60}$NWs without their alteration of cellular morphology.

### 4.2 Biodegradation of $C_{60}$NWs

After the long-term co-culture of macrophage-like cells and $C_{60}$NWs, decomposed $C_{60}$NWs were observed in the cells and the number of short (less than 3.0 μm in length) $C_{60}$NWs increased. In addition, the change of $C_{60}$NWs' morphology was observed after the co-culture with the macrophage-like cells. It is unlikely that these observed substances were composed of the materials derived from the culture medium and washing buffer, because a sufficient amount of water was used for the final wash of $C_{60}$NWs after the treatment with the enzyme in order to decompose the macrophage-like cells and these

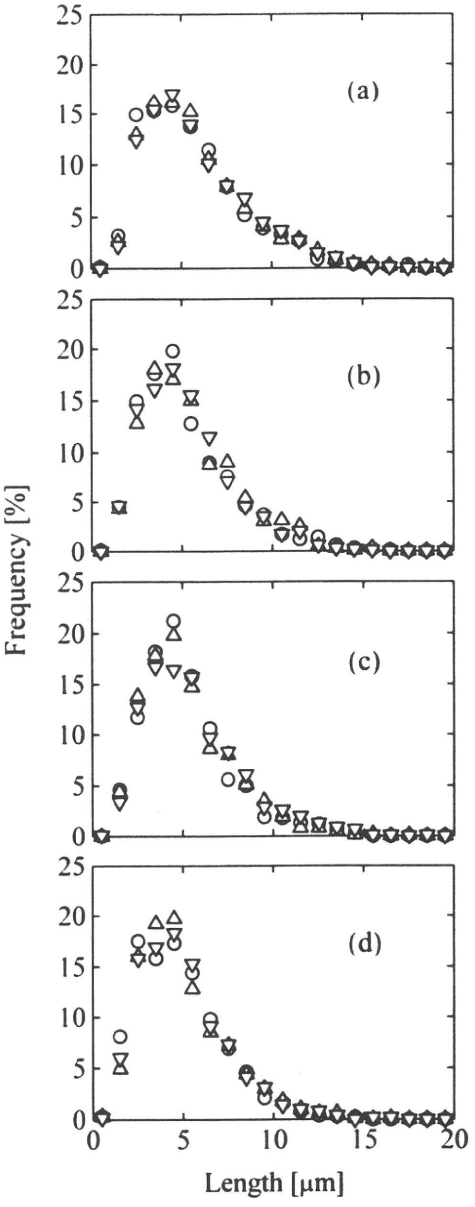


**Fig.5.** Length distribution of $C_{60}$NWs. (a) immediately after the exposure of culture medium to $C_{60}$NWs, (b) immediately after the exposure of macrophage-like cells to $C_{60}$NWs, (c) 28 days after the exposure of culture medium to $C_{60}$NWs and (d) 28 days after the exposure of macrophage-like cells to $C_{60}$NWs. The length was measured by an optical microscope after the enzymatic treatment and washing on the cell culture insert. Each symbols were expressed by measuring the length of about 1000 $C_{60}$NWs.

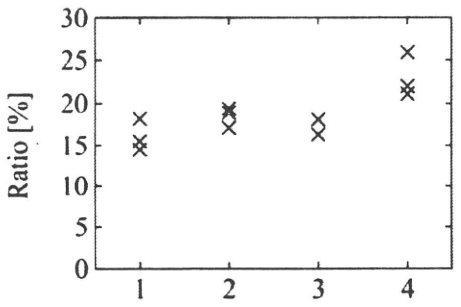


**Fig.6.** The ratio of short (less than 3.0 μm in length) $C_{60}$NWs. 1: Immediately after the exposure of culture medium to $C_{60}$NWs (Fig. 5 (a)). 2: Immediately after the exposure of macrophage-like cells to $C_{60}$NWs (Fig. 5 (b)). 3: 28 days after the exposure of culture medium to $C_{60}$NWs (Fig. 5 (c)). 4: 28 days after the exposure of macrophage-like cells to $C_{60}$NWs (Fig.5 (d)). Each point was expressed by measuring the length of about 1000 $C_{60}$NWs.

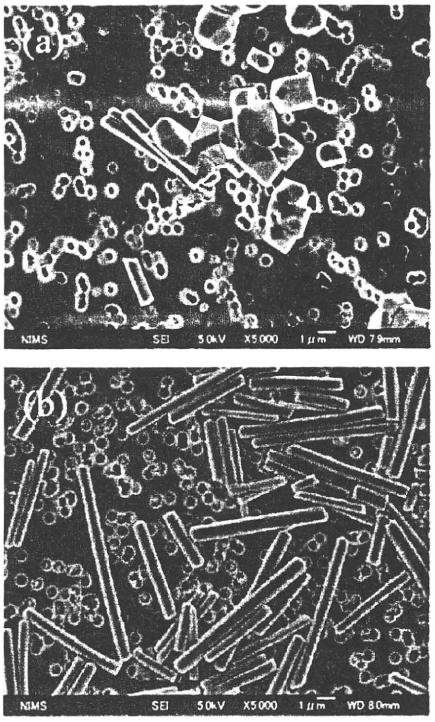


**Fig.7.** SEM images of the substances on the cell culture insert after the 28 days' exposure of (a) the macrophage-like cells and (b) the culture medium to $C_{60}$NWs.

substances were not observed at the control experiment. Hence, it is suggested that these substances are composed of fullerene molecules derived from the $C_{60}$NWs. It is considered that the macrophage-like cells decompose $C_{60}$NWs into individual $C_{60}$ molecules and that those observed granular substances must have recrystallized from these $C_{60}$ molecules via a dissolution-recrystallization process during the long-term co-culture or upon the enzymatic treatment.

These results suggest that the $C_{60}$NWs may decompose into individual $C_{60}$ molecules by macrophages owing to the weak van der Waals bonding forces acting between the $C_{60}$ molecules of $C_{60}$NWs. On the basis of this assumption, the $C_{60}$NWs may exert the effect which is not similar to that of the needle-like structure but is similar to that of fullerene molecules on organisms. Previous studies have reported that $C_{60}$ (the aggregate size was not described or larger than 1 μm) were nontoxic against mammalian cells [10, 11, 12]. The $C_{60}$NWs may also be nontoxic against organisms. Hence, the $C_{60}$NWs are expected for various applications not only in the engineering fields but also in the biological field such as drug delivery systems and tissue engineering.

In this study, we demonstrated that the macrophage-like cells decompose $C_{60}$NWs. However, the mechanism is not clear. Recent studies show human neutrophils generate not only reactive oxygen species but also ozone in bacterial killing and inflammation [13, 14]. Additionally, there has been considerable research on the THP-1 [15]. We are going to carry out further research on the biodegradation mechanism of $C_{60}$NWs by the macrophage-like cells and on the biological impact (cell viability, LDH, cytokines, active oxygen and ozone generation, and so on) of $C_{60}$NWs using short and long $C_{60}$NWs.

## 5 Conclusion

The interaction between macrophage-like cells and $C_{60}$NWs was investigated in this study. Macrophage-like cells were exposed to 10 μg/mL of $C_{60}$NWs with an average length of about 6.0 μm and an average diameter of 660 nm. The macrophage-like cells internalized the $C_{60}$NWs with time and more than 70% of the cells internalized the $C_{60}$NWs after 48-h exposure. After the long-term co-culture, decomposed $C_{60}$NWs were observed in the macrophage-like cells and the number of short (less than 3.0 μm in length)

$C_{60}$NWs increased after the exposure. These results suggest that macrophages can decompose $C_{60}$NWs into individual $C_{60}$ molecules as the primary immune response.

## Acknowledgment

Part of this work was supported by NIMS Center for Nanotechnology Network.

*References:*

[1] K. Miyazawa, Y. Kuwasaki, A. Obayashi and M. Kuwabara, $C_{60}$ nanowhiskers formed by the liquid-liquid interfacial precipitation method, *Journal of Materials Research*, Vol.17, No.1, 2002, pp.83-88.

[2] C. A. Poland, R. Duffin, I. Kinloch, A. Maynard, W. A. H. Wallace, A. Seaton, V. Stone, S. Brown, W. Macnee and K. Donaldson, Carbon nanotubes introduced into the abdominal cavity of mice show asbestos-like pathogenicity in a pilot study, *Nature Nanotechnology*, Vol.3, 2008, pp.423-428.

[3] K. Donaldson, R. Aitken, L. Tran, V. Stone, R. Duffin, G. Forrest and A. Alexander, Carbon Nanotubes: A Review of Their Properties in Relation to Pulmonary Toxicology and Workplace Safety, *Toxicological Sciences*, Vol.92, No.1, 2006, pp.5-22.

[4] J. P. Ryman-Rasmussen, M. F. Cesta, A. R. Brody, J. K. Shipley-Phillips, J. I. Everitt, E. W. Tewksbury, O. R. Moss, B. A. Wong, D. E. Dodd, M. E. Andersen and J. C. Bonner, Inhaled carbon nanotubes reach the subpleural tissue in mice, *Nature Nanotechnology*, Vol.4, 2009, pp.747-751.

[5] R. O. McClellan and T. W. Hesterberg, Role of Biopersistence in the Pathogenicity of Man-made Fibers and Methods for Evaluating Biopersistence: A Summary of Two Round-table Discussions, *Environmental Health Perspectives*, Vol.102, No.Supplement 5, 1994, pp.277-283.

[6] S. Tsuchiya, Y. Kobayashi, Y. Goto, H. Okumura, S. Nakae, T. Konno and K. Tada, Induction of Maturation in Cultured Human Monocytic Leukemia Cells by a Phorbol Diester, *Cancer Research*, Vol.42, 1982, pp.1530-1536.

[7] S. Nudejima, K. Miyazawa, J. Okuda-Shimazaki and A. Taniguchi, Observation of phagocytosis of fullerene nanowhiskers by PMA-treated THP-1 cells, *Journal of Physics: Conference Series*, Vol.159, 2009, pp.012008.

[8] Y. Tabata and Y. Ikada, Effect of the size and surface charge of polymer microspheres on their phagocytosis by macrophage, *Biomaterials*, Vol.9, 1988, pp.356-362.

[9] A. E. Porter, K. Muller, J. Skepper, P. Midgley, M. Welland, Uptake of $C_{60}$ by human monocyte macrophages, its localization and implications for toxicity: Studied by high resolution electron microscopy and electron tomography, *Acta Biomaterialia*, Vol.2, 2006, pp.409-419.

[10] S. Fiorito, A. Serafino, F. Andreola, P. Bernier, Effects of fullerenes and single-wall carbon nanotubes on murine and human macrophages, *Carbon*, Vol.44, 2006, pp.1100-1105.

[11] F. Moussa, P. Chretien, P. Dubois, L. Chuniaud, M. Dessante, F. Trivin, P. Y. Sizaret, V. Agafonov, R. Ceolin, H. Szwarc, V. Greugny, C. Fabre, A. Rassat, The Influence of $C_{60}$ Powders on Cultured Human Leukocytes, *Fullerene Science & Technology*, Vol.3, No.3, 1995, pp.333-342.

[12] T. Baierl, E. Drosselmeyer, A. Seidel and S. Hippeli, Comparison of immunological effects of Fullerene $C_{60}$ and raw soot from Fullerene production on alveolar macrophages and macrophage like cells in vitro, *Experimental and Toxicologic Pathology,* Vol.48, 1996, pp.508-511.

[13] P. Wentworth Jr., J. E. McDunn, A. D. Wentworth, C. Takeuchi, J. Nieva, T. Jones, C. Bautista, J. M. Ruedi, A. Gutierrez, K. D. Janda, B. M. Babior, A. Eschenmoser, R. A. Lerner, Evidence for Antibody-Catalyzed Ozone Formation in Bacterial Killing and Inflammation, *Science,* Vol.298, 2002, pp.2195-2199.

[14] K. Yamashita, T. Miyoshi, T. Arai, N. Endo, H. Itoh, K. Makino, K. Mizugishi, T. Uchiyama and M. Sasada, Ozone production by amino acids contributes to killing of bacteria, *Proceedings of the National Academy of Science of the United States of America,* Vol.105, No.44, 2008, pp.16912-16917.

[15] The FANTOM Consortium and the Riken Omics Science Center, The transcriptional network that controls growth arrest and differentiation in a human myeloid leukemia cell line, *Nature Genetics,* Vol.41, No.5, 2009, pp.553-562.

SYMPOSIUM PRESENTATION

# Risk Assessment Studies of Nanomaterials in Japan and Other Countries

**Hiroyuki Tsuda**

## Abstract

**Recent developments in nanoparticle (NP) technology and their commercial production have raised concern regarding NP risk to health and the environment. The toxicological characteristics of NP may not be similar to that observed in pre-NP materials because of the enormous differences in size and surface area. Thus, careful risk evaluation studies are required. Since some NP have already been produced and introduced into the market, before a suitable framework enabling risk management has been firmly established, toxicological studies based on the specificity of NP which are not subordinate to their commercial production are indispensable. The summary of nanotoxicology studies shown below clearly indicates that compared with the UK, EU, USA, and other countries, Japanese studies regarding metals and SWCNT are far from sufficient to evaluate risk.**

**Key Words:** Nanoparticles - toxicology - carcinogenicity - titanium dioxide - carbon black

*Asian Pacific J Cancer Prev,* **10,** DIMS Supplement 11-12

## Introduction

The safety of our living environment can be secured by the balanced function of three elements: risk assessment, risk management and risk communication. The first of these elements, risk assessment, must be addressed first, since without reliable risk assessment, risk communication and risk management can not function. Importantly, for reliable risk assessment long-term animal studies are indispensable.

These principles, of course, hold true for engineered nanoparticles. Unfortunately, the risk assessment data for engineered nanoparticles are rather fragmentary. However, the available findings do present a disturbing picture of potential carcinogens entering the market place. Engineered nanoparticles included in this review include nano-size titanium dioxide ($nTiO_2$), carbon black (nCB), single-walled carbon nanotubes (SWCNT), multiple-walled carbon nanotubes (MWCNT) and fullerenes (C60). A summary of the testing so far performed shows that data are limited and Japan is not putting the priority this subject deserves (see Table 1) and Tsuda et al (2009), for a review.

**Table 1. Number of Subacute/Chronic Toxicity Tests (PubMed, ~2007)**

| | ● | ■ | ▤ | Total |
|---|---|---|---|---|
| $TiO_2$ | 1 | 2 | 2[a] | 5 |
| S/MW-CNT | 2 | | | 2 |
| Fullerenes | | 1 | | 1 |
| Uf-Carbon black | | | 4[a] | 4 |
| Total | 0 | 3 | 6 | 9 |

[a]Carcinogenic

## Overall Evaluation and Proposal for the Future

During the development and marketing of nanomaterials, risk assessment of these new products has been perfunctory at best. While nanomaterials have undeniable benefits, their use also has undeniable potential risk. This risk must be addressed in an unbiased and thorough manner. Only after the toxicity of the various nanomaterials is understood can their true benefits be realized.

In rodent studies, $nTiO_2$ whether administered by inhalation or intratracheal instillation was shown to induce lung tumors with characteristic squamous cell morphology in female rats. These nanomaterials did not induce lung tumors in male rats. Our own studies have also shown that instillation of $nTiO_2$ into the lungs of female rats showed tumor promoting activity and resulted in elevated ROS-mediated damage and production of inflammatory cytokines. It is reasonable to assume that other metal-derived nanoparticles, such as aluminium and copper nanoparticles, and metal containing nanoparticles, for example nCB-metal mixtures and SWCNT and MWCNT preparations, are also capable of producing these effects.

*Nanotoxicology Project, Department of Molecular Toxicology, Nagoya City University Graduate School of Medical Sciences 1 Kawasumi, Mizuho-cho, Mizuho-ku, Nagoya 467-8601, Japan*

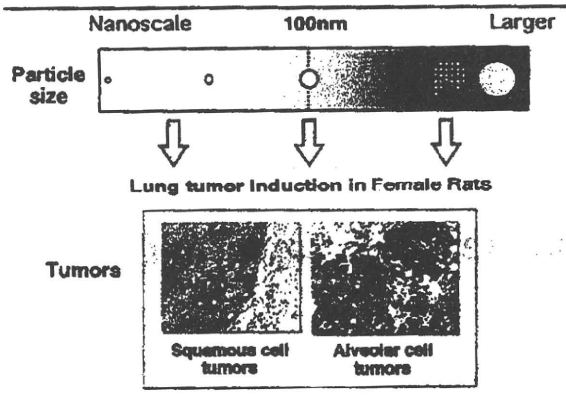


**Figure 1. Schematic Presentation of Carcinogenic Effects of $TiO_2$, Carbon Black.** Carcinogenic effects were elicited by both nano-scale and larger sized particles

Nanoparticles such as $nTiO_2$, nCB, SWCNT and MWCNT when intratracheally administered, were detected by light microscope as aggregates or agglomerates and these forms are reported to induce foreign body granulation tissue with various degree of inflammatory reaction. Although the relevance of foreign body-induced chronic inflammation to carcinogenesis is not clearly established, it is possible that reactive oxygen species (ROS) produced by macrophages attempting to destroy the foreign material in the inflammation site may cause DNA damage associated with carcinogenesis. Another possible contributing factor is metal, for example from metal-derived nanoparticles such as $TiO_2$ or from metal contaminants: these metals could also be involved in ROS production. Thus, it is possible that the observed carcinogenic effect is not specific to nanoparticles but rather associated with their ability to induce persistent foreign body-induced chronic inflammation and/or introduce metals into susceptible sites. For example, $TiO_2$ and carbon blacks larger than 100nm in diameter are known to induce lung tumors including similar squamous cell morphology (Nikula, 2000); (Pott and Roller, 2005) and both of these materials (larger than nano size) are classified as into group 2B (possibly carcinogenic to humans) by WHO/IARC (see Figure 1).

Mechanisms for mesothelioma induction by MWCNT in mice and rats have not been elucidated yet. A possible contributing factor is metal: Transition metals, such as iron, are commonly used as a catalytic center in the formation of CNTs, and contaminating metal in SWCNT and MWCNT particles could catalyze the formation of ROS by the Fenton reaction (Liu and Okada, 1994). One example of this type of toxicity is that human keratinocytes exposed to SWCNT were killed by ROS in the media (Shvedova et al., 2003). Another possible contributing factor is the length of the MWCNT (Pott and Roller, 2005; Muller et al., 2009; Sakamoto et al., 2009).

As noted at the beginning of this review, for reliable risk assessment long-term animal studies are indispensable. This is particularly true for risk assessment of potential carcinogens. The standard for the evaluation of the carcinogenic potential of a test chemical is testing in two rodent species, generally rats and mice, of each sex, at 3 doses (0, low and high) of the test chemical for up to two years. In the studies conducted to date concerning the carcinogenic risk presented by nanoparticles, there is a noticeable lack of long term testing: No long-term tests of any type have been reported for either SWCNT or fullerenes. Importantly, the primary goal of risk assessment is not to simply ban a product from the market place, but rather to determine product safety and establish guidelines lines for its production and use and promote consumer confidence. Given the known ability of many nanomaterials to induce mechanisms which are active in humans that are risk factors for carcinogenesis, for example ROS and inflammatory cytokine production, the continued introduction of these materials into the market is alarming. Establishing the safety of these materials is urgently needed.

In this short review, available in vivo data concerning the carcinogenic effects of $nTiO_2$, nCB, SWCNT and MWCNT, and Fullerenes is outlined. Of these, $nTiO_2$ and nCB are classified as possibly carcinogenic to humans. Testing of the carcinogenic activity of MWCNT produced mixed results. SWCNT and fullerenes have no carcinogenic activity in the studies conducted to date, however, toxicity testing of these materials has been quite limited and both of these materials have the potential to produce ROS. The observations noted here may apply to possible carcinogenic risk of other nanoparticles because of shared mechanisms of induction of inflammatory lesions and ROS generation. Our conclusions are that nanoparticles are clearly potentially toxic/carcinogenic to humans and their toxicity must be assessed, and their production and use managed appropriately.

## References

Liu M, Okada S (1994). Induction of free radicals and tumors in the kidneys of Wistar rats by ferric ethylenediamine-N,N'-diacetate. *Carcinogenesis*, **15**, 2817-21.

Muller J, Delos M, Panin N, et al (2009). Absence of carcinogenic response to multiwall carbon nanotubes in a 2-year bioassay in the peritoneal cavity of the rat. *Toxicol Sci*, **110**, 442-8.

Muller J, Huaux F, Moreau N, et al (2005). Respiratory toxicity of multi-wall carbon nanotubes. *Toxicol Appl Pharmacol*, **207**, 221-31.

Nikula KJ (2000). Rat lung tumors induced by exposure to selected poorly soluble nonfibrous particles. *Inhal Toxicol*, **12**, 97-119.

Pott F, Roller M (2005). Carcinogenicity study with nineteen granular dusts in rats. *Eur J Oncol*, **10**, 249.

Sakamoto Y, Nakae D, Fukumori N, et al (2009). Induction of mesothelioma by a single intrascrotal administration of multi-wall carbon nanotube in intact male Fischer 344 rats. *J Toxicol Sci*, **34**, 65-76.

Shvedova AA, Castranova V, Kisin ER, et al (2003). Exposure to carbon nanotube material: assessment of nanotube cytotoxicity using human keratinocyte cells. *J Toxicol Environ Health A*, **66**, 1909-26.

Tsuda H, Xu J, Sakai Y, Futakuchi M, Fukamachi K (2009). Toxicology of engineered nanomaterials - A review of carcinogenic potential.. *Asian Pacific J Cancer Prev*, **10**, 975-80..

特集

環境リスク

# ナノテクノロジーと環境リスク

西村　哲治

公　衆　衛　生
第74巻　第4号 別刷
2010年4月15日　発行

医学書院

# ナノテクノロジーと環境リスク

西村 哲治

## はじめに

20世紀後半のマイクロテクノロジーの世界から，21世紀はナノ(1 nm：1 mの10億分の1)テクノロジーの世界になると言われ，ナノメートルサイズのスケールで現象を理解し，物質の構造や配列を制御し，ナノメートルサイズの物質を取り扱うことにより，新しい性質や機能を利用した技術革新が期待されている．ナノサイズの物質(ナノ物質)はナノテクノロジーの重要な役割を担う新規物質・材料と考えられる．このナノサイズの物質を材料(ナノ材料)として取り扱おうとしている分野は多岐にわたっており，すでにわれわれの身の回りの一般家庭用品や食品にも使用されてきている．今後その適用範囲は拡大していくものと思われる．これらの製品を使用することで，われわれがナノ材料に直接接する機会が増加すると共に，使用後の廃棄物から環境中への放出が予想され，環境リスク評価への関心が高まっている．

本稿では，工業用に生産，使用されるナノ材料に焦点を当てて，環境リスクについて概説する．なお，ジーゼル排ガス中に含まれるナノサイズの微粒子など，非意図的に生成されるナノ粒子に関しても重要な課題はあるが，ここでは割愛させていただく．

## ナノ材料の特性

### 1. ナノ材料の大きさ

工業用ナノ材料の大きさの定義は，OECDはじめ各分野で議論されているが，「長径が100 nm以下の粒径を有するもの」となっている．大きさが議論の的になっているのは，これまで取り扱ってきた同重量の材料に比べ表面積が大きくなることによる物理化学的影響が異なってくる可能性が考慮されているからである．例えば，他の物質との相互作用，反応性，化学物質の吸着性が高まるのではないかと考えられている．また，機械的，光学的，磁気的，電気的，生物学的な特性も異なっていることが考えられる．これらの観点から，これまでの有害影響は化学的性状を中心として評価されてきたが，その他，物理的な側面等からも考慮しなくてはいけないと考えられている．

一方，人への健康影響を含む生態系への影響を考慮する際に，工業用ナノ材料の単分子がナノサイズであっても，製品中または環境中でナノサイズの粒子として存在し，どの大きさの粒子として挙動するかが大きな問題となる．一例として，化粧品に使用されている酸化チタンに関して，皮膚塗布による曝露評価をする際に分散溶液中の粒径分布を測定した結果を示す．アルミナ，シリカおよびシリコーンで表面修飾した初期粒径35 nmの酸化チタン(ルチル型：酸化チタン含量80%以上)を，良い分散を示すシリコーンに超音波処理

にしむら てつじ：国立医薬品食品衛生化学部　連絡先：〒158-8501 東京都世田谷区上用賀1-18-1

した場合においても，単分子として存在する割合は低く，平均689 nm(分散中央の径：778 nm)の凝集した塊の粒径分布を示した(五十嵐，私信)．

この結果から，提供された製品中のナノ材料の初期粒子径がナノサイズであっても，環境中に放出された後には凝集状態で挙動する可能性が高いと推測される．

一方，有害影響を考える場合は，凝集塊を形成していても，単分子もしくは数分子のナノサイズの粒子が接触，吸収される可能性，吸収後に単分子として体内循環をする可能性も考慮に入れておかなくてはならない．これらのことをどのように考えるかについて，国際的な共通認識はまだできていないと思われるが，われわれは，できるだけ提供された状態を尊重した上で，ナノ粒子としての影響を評価するために，ナノサイズの分散系を作製して検討を進めることとしている．

### 2. ナノ材料の安定性

ナノ材料と言っても，その素材は金属類，炭素，鉱物類のほか，リポソーム類のような生体成分により構成されているものもあり，安定性に大きな差がある．リポソームはリン脂質で構成された人工膜でできた球状をしており，体内に取り込まれたとしても長期間安定して存在することは考えにくい．また，環境中においても同様に，比較的短期間に分解されることが予想される．

一方，金属類，炭素，鉱物類については単体の構成成分自体の安定性は高く，体内や環境中における半減期は長いものが多いと考えて良いであろう．鉱物を素材とするものは，元来天然の素材であることから，天然に存在する粒径よりも微小な粒子が大量に放出されて影響を及ぼすことに注意を払う必要がある．金属類では，環境中でイオンになることも考慮に入れなくてはならない．また，炭素素材のナノ物質は，高温でないと分解しにくいものが多い．

このように，ナノ物質と総称される中には素材や形態により安定性が大きく異なっているものが混在していることを理解し，使用方法なり環境中における循環に，十分な配慮をしなくてはならない．

環境中に放出された後，また体内に吸収された後，ナノ材料がどのような挙動をとるか推定することが次の課題である．前述したように，単分子として存在するよりも，複数の単体が凝集した状態で標的器官に貯留・蓄積していることも考えなくてはいけない．

## 環境からの曝露

環境リスクを評価するためには，対象とするナノ物質料の特性と使用範囲，ヒトおよび環境の到達点にいたる経路を理解する必要がある．

曝露の発生源は，ナノ物質を製造，使用する作業環境からの放出・曝露がある．また，ナノ物質が使用されている製品からの放出・曝露も考えられる．例えば，化粧品に含まれるナノ物質は意図的に使用され，洗浄した結果，水環境への排出がある．さらに，それらの一般家庭用品を廃棄した廃棄物処理場からの放出も考慮しなければならないであろう．

排出されたナノ材料は，空気，水，土壌を経由して環境中を移動し，環境中に存在する様々な物質と相互作用を及ぼし合いながら，最終到達点に集積していくであろう．環境中の挙動については，化学物質やジーゼル排出微粒子のこれまで蓄積された情報により推定できる所はあるであろう．しかし，凝集状態や，水や土壌中の天然に存在する物質等との相互作用については，十分な情報を得ることも課題である．

生態系生物に対する影響は，前述したようなナノ物質の物理化学的な特性に加え，環境中の残留性，生物蓄積性に依存することはこれまでの化学物質の研究から推測されるが，現在のところ個体に対する影響に関するデータが十分でない．環境中における挙動と最終到達点を明らかにすることにより，いずれの環境媒体に汚染が進むかを理解し，リスクを受ける可能性の高い生物種集団に対する影響を検討することが必要である．人間も生態系生物であり，生態系生物の均衡と恵みにより，直接・間接的に影響を受けることを考慮しなくてはならない．

## 曝露評価

### 1. 検出法

環境リスク評価を行う際，有害影響評価と対をなす曝露評価が重要である．そのためにも，環境中および生物試料中のナノ物質を同定・定量するための分析方法の確立が緊急の課題である．粒径や溶解性により，環境の大気，水，土壌から効率よく抽出できる適切な前処理方法の確立も検討すべき課題がある．

対象のナノ材料が，影響発現部位もしくは作用を及ぼすと想定される部位に存在することを示すことが必要である．例えば，金属ナノ粒子は，組織を硝酸加熱分解後，燃焼灰化した試料中から溶解した金属元素の量を機器分析により同定・定量する方法がある．酸化チタンの場合は，対象臓器0.1 g を裁断し，硝酸/過酸化水素水(3：1)5 ml と精製水 2 ml を加え，600 W，圧力 80 PSI で 20 分間マイクロ波照射し，2 分間保持した後，20 ml に定溶して試料溶液とする．誘導結合プラズマ-質量分析計(ICP-MS)に注入して得られるピーク面積を測定し，チタン標準液を用いて作成した検量線から試料溶液中のチタン濃度(ppb，ng/ml)を求め，酸化チタン量に換算し，臓器中の酸化チタン量(mg/g)を求めている．金属類に関しては，同様な手法で測定はできるが，炭素を成分とするフラーレン C60 やカーボンナノチューブでは ICP/MS を用いることはできない．フラーレン C60 は水に溶けにくく，トルエンやキシレンなどの限られた有機溶媒にのみ溶解する物質である．

そこで，われわれは，対象組織をドデシル硫酸ナトリウム(SDS)で溶解した後，トルエンで抽出し，液体クロマトグラフ-タンデム質量分析計で測定する方法を採っている[1]．試料の相違による抽出効率を評価するために，同様の挙動をとるフラーレン C70 を抽出に加えて，抽出効率補正に使用している．しかし，これらの方法では，ナノ材料の存在や量を評価することは可能であるが，実際にナノの状態で存在しているのか，あるいは凝集しているのか，別の形態で存在しているのかを把握することはできない．最終的には，多くのナノ材料は凝集塊を形成するため，電子顕微鏡による生体組織中の存在の確認が必要となってくる．しかし，電子顕微鏡で見ることが困難なサイズ状態のナノ材料の存在については証拠は得られない．

これを補う方法として，対象物質に標識で修飾する方法が採用されている．例えば，放射性同位元素の使用，蛍光物質の修飾などがあるが，製造や同定に制限があること，付点や，修飾することによる挙動の変化の有無を否定できない点が課題となっている．一方，カーボンナノチューブについては，機器による定量分析が困難であり，前処理後の試料を透過型電子顕微鏡により，本数や形態を手動で計測する以外に確実に測定する方法がない状況である．今後，感度良く，精度の高い検出方法を確立しなくてはならないであろう．

### 2. 空気媒介の曝露

ヒトへの吸入曝露は空気を媒体とするのが，現在のところ最も可能性が高い曝露経路である．一般的な生活環境における吸入曝露の可能性はあまりないと考えられるが，ナノ物質の製造・加工・使用する作業場において，曝露される可能性が大きいことが推測される．作業環境における空気経由のほか，皮膚経由の職業曝露と健康影響も配慮されなければならず，曝露を減少させる技術開発と利用は重要な課題である．

これまで，金属，鉱物，排ガス粒子などの微粒子の吸入曝露研究は数多く行われてきており，過去の知見はナノ物質の影響を検討するために有用である．しかし，実際に影響を検証しようとする際には，ナノ物質の特性である凝集しやすい性質から凝集塊を形成した結果生じる，肺組織中の細気管支等を詰まらせることによる物理的な二次影響を見るという課題が残されており，現在のところナノ物質の影響に対する知見は限られている．繊維状粒子については，アスベストやアスベスト代替物である人工繊維による研究で蓄積された知見が有益であろう．

特集

### 3. 水および土壌媒介の曝露

水もしくは土壌を介してナノ物質に曝露することに直接的な証拠はほとんどなく，また，水環境中の挙動は不明なことが多い．ナノ物質を実験動物もしくは *in vitro* 試験で界面活性物質や媒体に結合させて投与溶液を調製していることから，浄水処理が施されている飲料水などによる直接的な曝露は少ないと考えられる．魚介類や土壌中生物類により取り込まれる可能性，それを摂食することによる経口曝露が考えられるが，知見はほとんどない．

### 4. 意図的な曝露

ナノ材料は一般家庭用品，化粧品や食品に使用されている．これらから経口もしくは経皮曝露する可能性がある．われわれの検討結果では，化粧品に使用されている粒径の酸化チタン(ルチル型)をラットの健全な皮膚へ反復塗布した後の皮膚の電子顕微鏡観察において，酸化チタンナノ粒子は角質層にとどまり，毛包部分を含め表皮，真皮層にまで透過するような像は認められなかった．また，一般状態，体重および摂餌量は対照群と試験群間で変化はなく，臓器重量についても群間で有意な差は認められなかった．血液および病理的検討においても，肝臓，腎臓，脾臓等各臓器のチタン濃度は，酸化チタン塗布群と対照群とでほとんど差は認められなかった．

一方，コーン油に溶解したフラーレン C60 を強制経口投与した結果，糞便から投与の 85% 以上に当たるフラーレンが検出され，経口による吸収率が悪いことが示唆された．水溶性の $^{14}$C-水溶性フラーレンを経口投与した結果，大部分は糞便中に排泄されたとの報告もある[2]．

これらの結果は，限られた情報であるが，実際上使用される形態のナノ粒子は吸収されにくいことを示していると言えるであろう．しかし，今後，様々な形態や曝露状態を想定した評価情報を蓄積していくことが重要である．

## おわりに

ナノ物質はナノテクノロジーの中心的な新規開発物質として，急速に種類と生産量が増加しつつあり，われわれの生活空間での使用が多岐に亘り見込まれている．基本的な評価に関して，従来の化学物質と同様であると考えられるが，ナノ物質としての特有の性状から，これまでのリスク評価で用いられてきた技術や手法だけでは十分に評価しきれない可能性が指摘されている．

本稿で述べたように，情報の集積に努めなくてはならない課題もあり，今後，科学的な取り組みの上に，十分な議論と適正なリスクコミュニケーションを行っていくことが必要であろう．

## 文　献


1) 久保田領志，他：高速液体クロマトグラフィー—タンデム質量分析法による生物試料中フラーレンの分析法の開発．国立医薬品食品衛生研究所報告 **127**：65-68, 2009

2) Yamago S: *In vivo* biological behavior of a water-miscible fullerene; 14C labeling, absorption, distribution, excretion and acute toxicity, et al. Chem Biol **2**(6): 385-389, 1995

Cancer Science
The official journal of the Japanese Cancer Association JCA

# Age dependence of radiation-induced renal cell carcinomas in an Eker rat model

Toshiaki Kokubo,[1,2,3] Shizuko Kakinuma,[1] Toshiyuki Kobayashi,[2] Fumiko Watanabe,[1] Riichirou Iritani,[4] Kaori Tateno,[4] Mayumi Nishimura,[1] Tetsu Nishikawa,[3] Okio Hino[2] and Yoshiya Shimada[1,5]

[1]Experimental Radiobiology for Children's Health Research Group, Research Center for Radiation Protection, National Institute of Radiological Sciences, Chiba; [2]Department of Pathology and Oncology, Juntendo University School of Medicine, Tokyo; [3]Laboratory Animal Sciences Section, Department of Technical Support and Development, Fundamental Technology Center, National Institute of Radiological Sciences, Chiba; [4]Science Service Co., Chiba, Japan

(Received September 24, 2009/Revised November 8, 2009/Accepted November 15, 2009/Online publication February 8, 2010)

**Exposure to carcinogens early in life may contribute to cancer development later in life. The amount of radiation exposure children experience during medical procedures has been increasing, so it is important to evaluate the radiation risk of cancer in developing organs. Toward this goal, we assessed the risk of developing renal cell carcinoma using Eker rats as a kidney tumor model. F1 hybrids of male Eker (*Tsc2* mutant) and female F344 rats were irradiated with 0.5 or 2 Gy gamma radiation on gestation days 15 and 19, and on postnatal days 5, 20, and 49. At 27 weeks of age, kidneys were examined for proliferative lesions. Preneoplastic lesions such as phenotypically altered tubules increased after postnatal irradiation as a function of age-at-irradiation, and hyperplasia were greatly increased after perinatal and postnatal irradiation. In contrast, development of adenoma and adenocarcinoma were evident in animals irradiated at perinatal ages, being maximal at gestational day 19. The frequency of LOH at the *Tsc2* locus was unexpectedly low – 0% (0 of 4) for the unirradiated control, and 17% (6 of 35) for the irradiated group. Irrespective of LOH, the mTOR (mammalian target of rapamycin) pathway, which is negatively regulated by the Tsc1/2 complex, was activated in both benign and malignant lesions, as evidenced by phosphorylation of S6 ribosomal protein and 4E-BP1. This suggests that the wild-type *Tsc2* allele may be functionally inactivated. In conclusion, actively growing kidneys in perinatal-aged (F344 × Eker) F1 rats ($Tsc2^{+/-}$) are at risk for radiation-induced malignant transformation of the renal epithelium associated with mTOR activation. (*Cancer Sci* 2010; 101: 616–623)**

Approximately 2% of human cancers occur in the kidney. The leading known environmental risk factors for renal cancer are smoking, chemical exposure, asbestosis, obesity, hypertension, and end-stage renal disease.[1,2] It is reported that patients treated for ankylosing spondylitis and cervical cancer with therapeutic doses of radiation show an increased risk of developing renal cancers.[2] The risk of atomic bomb survivors developing renal cancer is minimal, however.[3] In view of the small number of radiation-associated renal cell cancers, it is difficult to draw any firm conclusions with regard to the effects of radiation.

Children are considered to be more sensitive to radiation than adults, and they have a longer period of opportunity for expressing radiation damage.[4] There are primarily two types of kidney tumor: Wilms' tumor (or nephroblastoma), and renal cell carcinoma. Using data from the Oxford Survey of Childhood Cancers, it was reported that *in utero* exposure to radiation increases the risk of Wilms' tumors by one and a half times,[5,6] although the data from atomic bomb survivors do not support the conclusion.[7] Experimentally, Wilms' tumor can be induced in rats by transplacental exposure to *N*-methyl-*N*-nitrosourea and *N*-ethyl-*N*-nitrosourea.[4,8,9] Susceptibility increases as the fetal kidney develops from day 14 to 18, during which time the mesenchymal–epithelial transition occurs as well as the active growing of comma- and S-shaped bodies, which produces podocyte progenitors and the precursors of tubule segments,[10] and, therefore, is an anlage of glomerular cavity and renal tubules. Susceptibility is rapidly lost after birth.[11] In contrast to Wilms' tumors, there is only sparse information available about the effect of developmental age on renal cell carcinogenesis.[12] The development of both hereditary and sporadic clear cell renal cell carcinoma, comprising over 80% of all renal cell carcinomas in humans, is a result of a mutation in the von Hippel–Lindau tumor suppressor gene, *VHL*, which renders the protein product inactive.[13] Mice that are heterozygous for *VHL* in the germ line, however, develop normally and show no phenotype of renal cell carcinoma and cannot therefore be used for experimentally induced carcinogenesis.[14] In contrast, Eker rats provide a unique model for studying the etiology of renal cell carcinomas. These rats carry an allele of the tumor suppressor gene, *Tsc2*, disrupted by viral insertion. Tuberin, the protein product of *Tsc2*, inhibits mTOR (mammalian target of rapamycin),[15] and the mTOR pathway has a critical function in regulating *Tsc2* tumor progression.[16,17] The resulting LOH in *Tsc2* for these rats thus leads to mTOR activation and development of renal cell carcinomas.[18,19] In humans, tuberous sclerosis complex (TSC) is caused by a loss-of-function mutation in either of two tumor suppressor genes, *TSC1* or *TSC2*. TSC is a dominantly inherited disease marked primarily by the formation of hamartomas in a wide variety organs.[20] Malignant tumors, such as renal cell carcinomas, also develop in TSC patients.[21]

In this study, we investigated the age-window for susceptibility to radiation-induced renal cell carcinogenesis using an Eker rat model. We found that the perinatal stage, when comma- and S-shaped bodies form (i.e. when glomerular anlage and renal tubules are actively developing), is the most susceptible period for induction of renal adenomas and adenocarcinomas. Although LOH at the *Tsc2* allele was as low as 15%, 100% of the tumors showed an activation of mTOR, which suggests functional loss of *Tsc2*.

## Materials and Methods

**Animals.** The rats used were F1 hybrids of male Eker rats and female Fischer-344 (F344) rats (CLEA Japan, Tokyo, Japan). Only F1 hybrids with the genotype of $Tsc2^{+/-}$ were used throughout this study. Genetic homogeneity of Eker rats was maintained in our laboratory by brother–sister mating. All animals were housed under specific pathogen-free conditions in autoclaved cages with sterilized wood chips, and were kept in a room with controlled temperature (23 ± 1°C) and humidity (50 ± 5%) under a regular 12-h light/12-h dark cycle. All

[5]To whom correspondence should be addressed. E-mail: y_shimad@nirs.go.jp



doi: 10.1111/j.1349-7006.2009.01456.x